Journal of Information & Computational Science 10:6 (2013) 1551–1558 April 10, 2013
Available at http://www.joics.com

A Calibration Method of Three-axis Magnetic Sensor Based on Ellipsoid Fitting

Wenguang Feng, Shibin Liu*, Shiwei Liu, Shanglin Yang

School of Electronics and Information, Northwestern Polytechnical University, Xi'an 710072, China

Abstract

It is very essential for a magnetic sensor to be calibrated before use because of various disturbances. However, Constrained by maneuverability of carriers, sample data distribute in a quite limited area, traditional calibration approach using ordinary least-square ellipsoid fitting algorithm makes large error or even cannot compensate properly. In this paper, a new onboard calibration method based on ellipsoid fitting is presented, without requiring external reference. Sample data are obtained in the restricted area by rotating carrier in three simple traces, ellipsoid coefficient are calculated using constrained least squares algorithm. The proposed method is contrasted with the traditional method via software simulation and experimental test; the results indicate that the new calibration method is stable and reliable, and superior to the traditional approach.

Keywords: Magnetic Sensor; Calibration; Ellipsoid Fitting; Constrained Least Square

1 Introduction

As a part of magnetic compass, three-axis magnetic sensor indicates the heading of carrier by measuring the Earth's magnetic field, and is widely used in aircraft, robots and other autonomous vehicles. Due to technological limitations in sensor manufacturing and influence of surrounding ferromagnetic elements [1], output data of sensor is distorted with various disturbances; therefore, it must be calibrated before use.

Many calibration techniques have been presented in the literature. A classic calibration method called swinging algorithm derived in [2] is based on the fact that the heading error is a Fourier function of the heading. However, this method is not convenient, as an external reference must be employed, and induces additional errors when the location of sensor changes, as calibrated result is related with the magnitude of the earth's magnetic field. A class of reference-free methods has been also proposed, which utilize linear least-square algorithm or iterative algorithm to estimate the parameters for a given data set. Linear least-square algorithms require a proper uniform distribution of the data over all attitudes [3, 4, 5], while iterative algorithms need large amount of computation and precise initial conditions [6, 7]. Furthermore, a sufficient attitude scope is

*Corresponding author.
Email address: liushibin@nwpu.edu.cn (Shibin Liu).

DOI: 10.12733/jics20101833

necessary for sample data collection in the aforementioned methods, which is not feasible for onboard applications, because it is very difficult to force sensor carrier to maneuver at all the needed attitude. For example, some kind of Unmanned Aerial Vehicle (UAV) can only fly at three attitudes for data acquisition, which are level flight, left-circling flight and right-circling flight, and the absolute value of pitch angle is usually less than 40° [8]. Therefore, a calibration method with constrained sample data is needed.

In this paper, a new onboard calibration method based on Constrained Least Squares Ellipsoid Fitting algorithm (CLSEF algorithm) is presented. The method uses the sample data collected at three attitudes of carrier, error coefficients are calculated by the least-square algorithm, which are used to correct the output data of magnetic sensor. A new constrained condition involved with the limited sample data is applied to achieve an accurate ellipsoid fitting. Magnetic sensor can achieve high precision by this method, without external reference and only relying on the limited sample data recorded on three flight routes.

2 Error Analysis and Modeling

For three-axis magnetic heading sensor, the error of output data mainly includes zero bias, scale factor, non-orthogonality error and deviations influenced by local magnetic interferences. The physical magnetic field vector in body coordinate frame is denoted as h_t, and the original output data vector of the sensor is denoted as h_s. Due to the presence of error, $h_s \neq h_t$, the relationship can be described as follows:

$$h_s = K_d K_p h_t + B_e = K_e h_t + B_e \tag{1}$$

where K_d is a 3-D diagonal matrix that represents the sensitivity of the sensor for each axis, K_p accounts for non-orthogonality of the sensor and part of soft iron errors which can be expressed with a lower triangular matrix according to the inherent reference coordinate system established in reference [1], B_e represents the null shifts and the hard iron errors.

Calibration is a process that corrects the known original output data vector h_s to the physical magnetic field vector h_t with the error coefficient matrices K_e and B_e using inverse derivation process of Eq. (1):

$$h_t = K_c(h_s + B_c) \tag{2}$$

where $K_c = K_e^{-1}$ and $B_c = -B_e$.

Within a fixed area, the magnitude of the physical magnetic field $\|h_t\|$ remains constant. When sensor rotates in direction, the locus of the physical magnetic field measured h_t is sphere:

$$\|h_t\|^2 = H^2 \tag{3}$$

where H represents the intensity of the local magnetic field. Substitute Eq. (2) into Eq. (3), and we have

$$h_s^T A h_s - 2b^T A h_s + b^T A b = H^2 \tag{4}$$

where $A = K_c^T K_c$ and $b = -B_c$.

Ellipsoid fitting-based calibration method supposes that the trajectory of original output data is ellipsoid, i.e. Eq. (4) represents an ellipsoid equation on vector h_s. Thus, calibration of sensor is to seek an ellipsoid fitting method to estimate the compensation coefficients of K_c and B_c.

3 Ellipsoid Fitting Algorithm

Since an ellipsoid is a kind of conicoid, its general equation can be represented as follows:

$$f(p) = a_1x^2 + a_2xy + a_3y^2 + a_4xz + a_5yz + a_6z^2 + a_7x + a_8y + a_9z + a_{10} = 0 \tag{5}$$

where $p(x, y, z) \in R^3$. Analyzing the correspondence relation between Eq. (4) and Eq. (5), we have

$$A = k \begin{bmatrix} a_1 & a_2/2 & a_4/2 \\ a_2/2 & a_3 & a_5/2 \\ a_4/2 & a_5/2 & a_6 \end{bmatrix} \quad \text{and} \quad b = -\frac{k}{2}[BA^{-1}]^T, \tag{6}$$

where $B = [a_7\ a_8\ a_9]$, and $k = (b^T Ab - H^2)/a_{10}$.

If we define α and ξ by

$$\alpha = [a_1, a_2, a_3, \cdots\ a_{10}]^T, \quad \xi = [x^2, xy, y^2, xz, yz, z^2, x, y, z,\ 1]^T,$$

Eq. (5) can be expressed in the compact form:

$$\xi^T \alpha = 0 \tag{7}$$

Ellipsoid fitting is to compute an optimal coefficient matrix α so that the ellipsoid fit data points as close as possible. Usually mean of sum of squares of the distances between data points and ellipsoid curve surface is deemed as fitting criteria. Given data points $p_i(x_i, y_i, z_i)$, $i = 1, 2, 3 \cdots N$, the objective function is

$$J = \frac{1}{N}\sum_{i=1}^{N} d_i^2 \tag{8}$$

where d_i represents the distance between the ith data point and ellipsoid. According to fitting algorithm [9, 10, 11, 12], we define

$$d_i = \sqrt{\frac{f(p_i)^2}{Df(p_i)^T Df(p_i)}} \tag{9}$$

where $Df(p_i) = \left(\frac{\partial f(p_i)}{\partial x}, \frac{\partial f(p_i)}{\partial y}, \frac{\partial f(p_i)}{\partial z}\right)^T$, and constraint by

$$\frac{1}{N}\sum_{i=1}^{N} Df(p_i)^T Df(p_i) = 1 \tag{10}$$

which satisfies

$$\frac{1}{N}\sum_{i=1}^{N} Df(p_i)^T Df(p_i) \approx Df(p_j)^T Df(p_j) \tag{11}$$

for $j = 1, 2, 3 \cdots N$. Then, expression (8) can be simplified to:

$$J = \frac{1}{N}\sum_{i=1}^{N} (f(p_i))^2 \tag{12}$$

Substitute expression (7) into expression (12) and (10), we have

$$J = \alpha^T C\alpha \tag{13}$$

$$\alpha^T Q\alpha = 1 \tag{14}$$

where $C = \frac{1}{N}\sum_{i=1}^{N}(\xi_i\ \xi_i^T)$, $Q = \frac{1}{N}\sum_{i=1}^{N} D(\xi_i)D(\ \xi_i)^T$.

Thus, ellipsoid fitting estimator (8) becomes a constrained optimization problem represented by expression (13) and (14). Let us consider the function:

$$\varphi(\alpha, \lambda) = \alpha^T C\alpha - \lambda(\alpha^T Q\alpha - 1) \tag{15}$$

using Lagrange multipliers theorem, we arrive at simultaneous equations as follows:

$$\begin{cases} C\alpha = \lambda Q\alpha & \text{(a)} \\ \alpha^T Q\alpha = 1 & \text{(b)} \end{cases} \tag{16}$$

As can be seen, problem expressed by (13), (14) becomes an ordinary eigenvalue problem, and the solution α is the generalized eigenvector of matrix C with respect to matrix Q corresponding to the smallest positive eigenvalue, which also satisfies the formula (16-b) [10].

Thereby, solving matrices A and b using the aforementioned ellipsoid fitting algorithm, determining the compensation coefficients K_c and B_c according to the relationship described in (4), we can calculate the error-free vector h_t.

4 Software Simulation

In order to evaluate the validity of the proposed algorithm, software simulation is performed to compare this method with the traditional method based on Ordinary Least Squares Ellipsoid Fitting algorithm (OLSEF algorithm) [4]. Suppose that the magnetic field is uniform at the location where the magnetic sensor is and its intensity is 0.52 Gauss. Magnetic sensor is installed on an UAV, and the flight trajectories are illustrated in Fig. 1, which include level, left-circling at a pitch angle of 30° and right-circling at a pitch angle of -30°. Spherical surface in the picture represents the geomagnetic field.

The error coefficient matrices are set respectively as follows:

$$K_e = \begin{bmatrix} 1.1338 & 0 & 0 \\ 0.0221 & 0.8537 & 0 \\ 0.0392 & -0.1271 & 0.9381 \end{bmatrix}, \quad B_e = \begin{bmatrix} 0.0159 \\ -0.0043 \\ 0.0016 \end{bmatrix}$$

and a Gaussian white noise with a variance σ of 0.00005 Gauss is added.

First, 360 positions are selected on each route at substantially uniform interval. The physical magnetic field vector h_s and the original output data vector h_t are collected, as shown in Fig. 2.

Second, Ellipsoid fitting is performed with the OLSEF algorithm and the CLSEF algorithm respectively, and error compensation coefficient matrices K_c and B_c are solved.

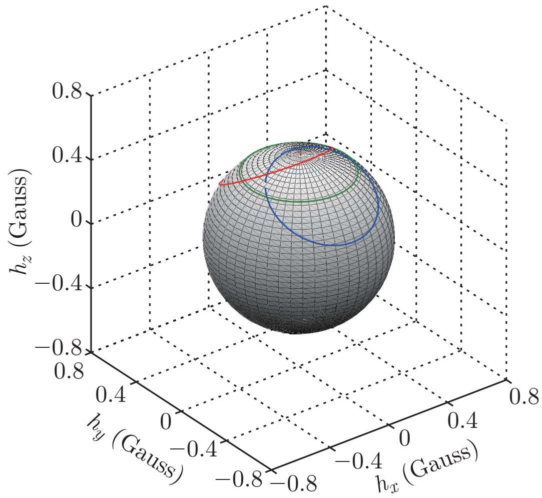

Fig. 1: Flight trajectories of simulation

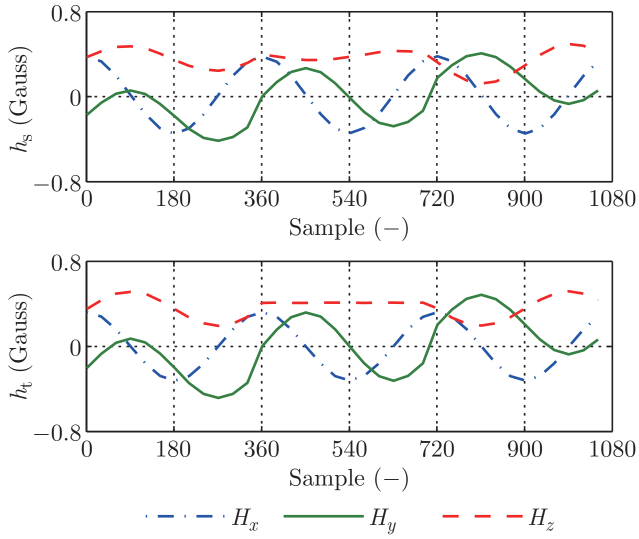

Fig. 2: Collected data vector

Finally, the physical magnetic vector h_s in Fig. 2 is corrected with error compensation coefficients, and the corrected heading is compared with the actual heading. The heading error ϕ_e is shown in Fig. 3 (a). After calibration, the maximum error of heading is diminished from 13.52° to 1.19° and 1.17°. To further assess the effect of calibration algorithms, all attitude data are compensated which are sampled for a pitch sweep interval of $\theta \in [-90,\ 90]°$, a roll sweep interval of $\gamma \in [-180,\ 180]°$ and unconstrained heading. The error of heading ϕ_e calculated is illustrated in Fig. 3 (b).

Fig. 3 (b) shows that, the maximum heading error is found to be 1.76° and 1.67°, whereas the maximum heading error before calibration is 20.04°. Due to the restriction of sample district, as distance from the three routes in Fig. 1 amplifies, heading angle error grows for both compensation algorithms; however, the CLSEF algorithm shows superior performance to OLSEF algorithm.

For statistical evaluation, we conducted the following experiments. 1000 independent noise instances for each σ with variances range from 0 to 0.0001 Gauss are generated. Data are sampled

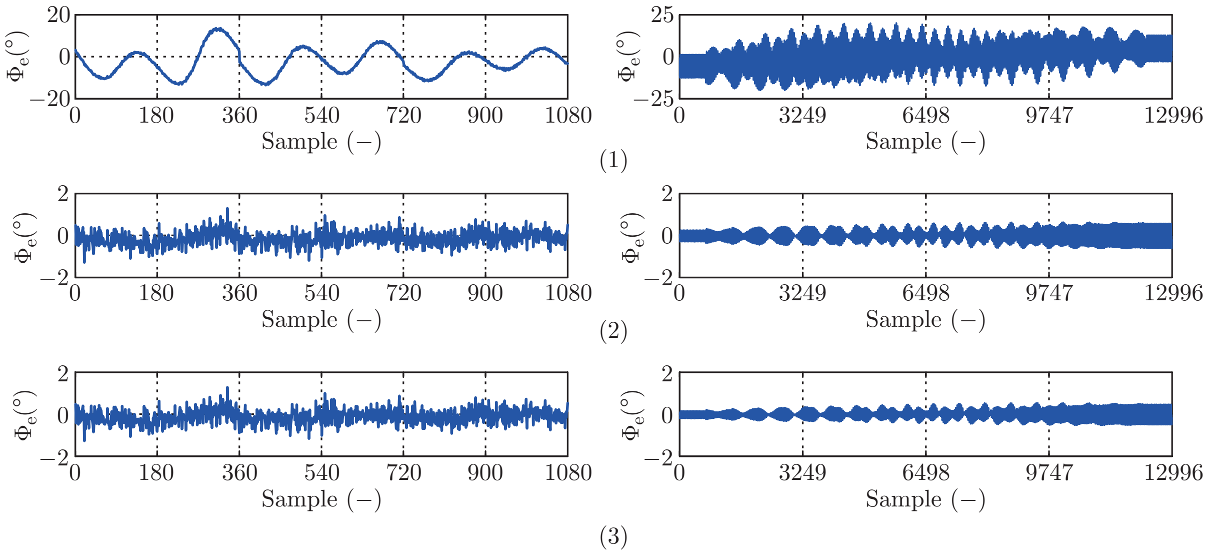

Fig. 3: Heading error of simulation. (1) Non-calibrated; (2) OLSEF algorithm; (3) CLSEF algorithm

along the routes in Fig. 1, and all attitude heading errors are recorded. Statistical averages B and deviations D are calculated as follows:

$$B = \left| \frac{1}{1000} \sum_{i=1}^{1000} \phi_{ie} \right|, \qquad D = \sqrt{\frac{1}{1000} \sum_{i=1}^{1000} \phi_{ie}^2},$$

where ϕ_{ie} represent the heading error of the ith recorded datum. The results are shown in Fig. 4 respectively.

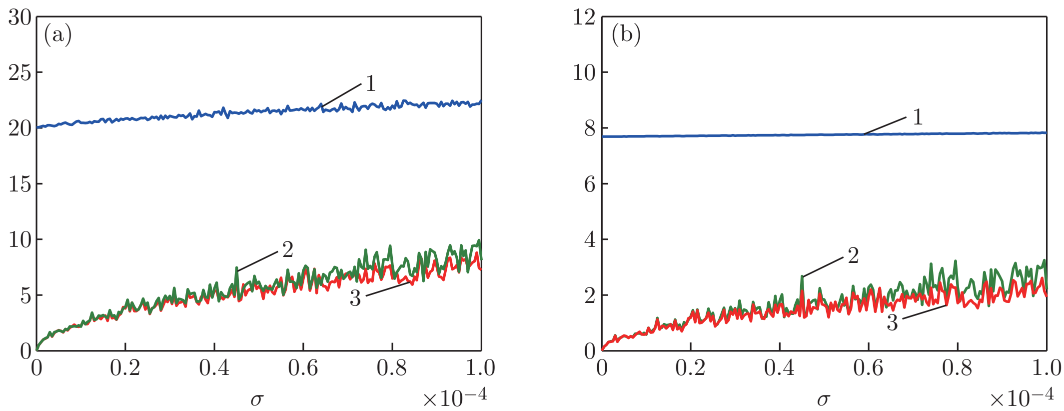

Fig. 4: The average (a) and Deviation (b) of the heading error. 1. Non-calibrated; 2. OLSEF algorithm; 3. CLSEF algorithm

As can be seen, heading error obtained with the calibration method based on the CLSEF algorithm is significantly superior to the error with calibration method based on the OLSEF algorithm, and with larger noise, the advantages are more obvious.

5 Experiments and Results Analysis

As a final verification, an experimental test is conducted. Magnetic sensor and nonmagnetic turntable are illustrated in Fig. 5. Magnetic sensor is fabricated in our laboratory [8], and turntable is 3SK-150 manufactured by the 6354 Institute of China Shipbuilding Industry Corporation, of which the resolution is 0.02°. Magnetic sensor is mounted with its x-axis precisely aligned with that of the turntable and its y-axis situated within the plane where the x and y axis of the turntable lies in, the turntable is located far away from magnetic materials.

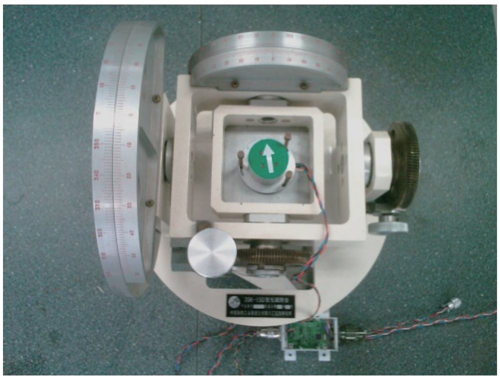

Fig. 5: Nonmagnetic turntable platform

First, routes are chosen according to the method mentioned in the last section, and twelve samples are taken on each route. Second, coefficients are figured out and transformed into error compensation coefficients matrices K_c and B_c. In the final step, compensation of sample data is performed; the heading error is calculated and depicted in Fig. 6.

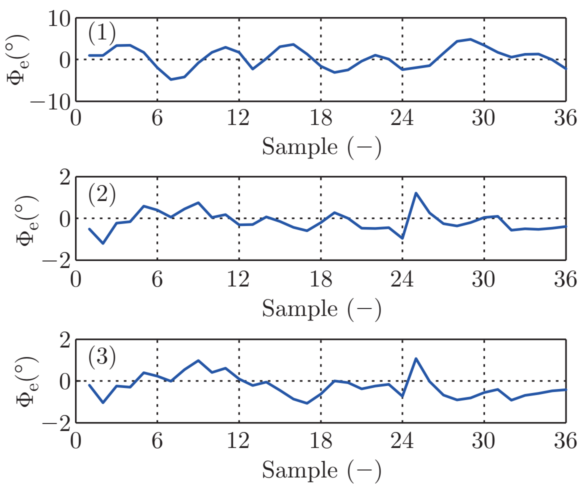

Fig. 6: Heading error of experiment. (1) Non-calibrated; (2) OLSEF algorithm; (3) CLSEF algorithm

The maximum error of heading before calibration is deduced as 4.82°, whereas the maximum heading error compensated by OLSEF algorithm is 1.20°, and the maximum heading error of CLSEF algorithm is 1.06° which shows higher precision.

6 Conclusion

Constrained by maneuverability of carriers, magnetic sensor cannot trace a wide range of attitude, therefore, traditional calibration method based on ordinary least square ellipsoid fitting algorithm cannot generate results with high accuracy. To cope with this problem, an alternative calibration method based on ellipsoid fitting is presented, which requires no external reference. The proposed method is theoretically studied, and compared with traditional approach via both software simulations and experimental tests. Simulation results indicate that, the new method is stable and reliable. Experiment results manifest that, the maximum value of heading errors with the new calibration method is 1.06° contrasted with 1.20° in traditional method.

References

[1] J. Veclak, P. Ripka, A. Platil et al., Errors of AMR compass and methods of their compensation, Sensors and Actuators A: Physical, 129 (2006), 53-57

[2] Demoz Gebre-Egziabher, Gabriel H. Elkaim, J. David Powell et al., Calibration of strapdown magnetometers in magnetic field domain, Journal of Aerospace Engineering, 19 (2006), 87-102

[3] J. M. G. Merayo, P. Brauer, F. Primdahl, J. R. Petersen et al., Scalar calibration of vector magnetometers, Meas. Sci. Technol., 11 (2000), 120-132

[4] Jiancheng Fang, Hongwei Sun, Juanjuan Cao et al., A novel calibration method of magnetic compass based on ellipsoid fitting, IEEE Transactions on Instrumentation and Measurement, 60 (2011), 2053-2061

[5] Nikos Grammalidis, Michael G. Strintzis, Head detection and tracking by 2-D and 3-D ellipsoid fitting, Proceedings of the International Conference on Computer Graphics, Geneva, Switzerland, 2000, 221-226

[6] Hui Yan, Changhan Xiao, Shengdao Liu et al., Horizontal error calibration method for triaxial fluxgate magnetometer, World Automation Congress, Hawaii, HI, 2008, 1-5

[7] J. F. Vasconcelos, G. Elkaim, C. Silvestre et al., A geometric approach to strapdown magnetometer calibration in sensor frame, IEEE Transactions on Aerospace and Electronic Systems, 47 (2011), 1293-1306

[8] Shi-bin Liu, Study on automatic magnetic deviation compensation of magnetic heading measurement for UAV, Acta Aeronautica et Astronautica Sinica, 28 (2007), 411-414 (in Chinese)

[9] Qingde Li, John G. Griffiths, Least squares ellipsoid specific fitting, Proceedings of Geometric Modeling and Processing, Beijing, China, 2004, 335-340

[10] Kenichi Kanatani, Prasanna Rangarajan, Hyper least squares fitting of circles and ellipses, Computational Statistics and Data Analysis, 55 (2011), 2197-2208

[11] Gabriel Taubin, Estimation of planar curves, surfaces, and nonplanar space curves defined by implicit equations with applications to edge and range image segmentation, IEEE transactions on Pattern Analysis and Machine Intelligence, 13 (1991), 1115-1138

[12] Ali Al-Sharadqah, Nikolai Chernov, Error analysis for circle fitting algorithms, Electronic Journal of Statistics, 3 (2009), 886-911